

Effectiveness of Lead Point with Microrecording for Determining STN-DBS in Parkinson Disease using HM-Models

Venkateswarla Rama Raju¹, Anuradha B², Sreenivas B³

¹Professor; ²Associate Professor; ³Asst. Professor; Dept. of Computer Science & Engineering, CMR College of Engineering & Technology, Medchal Rd Kanldakoya, Hyderabad, Telangana State 501401, India.

Abstract - Intraoperative microelectrode (signal) recording (MER) with deep brain electrical stimulator (DBS) for micro-electrode implantation in Parkinson's is a successful method for target nucleus localization for determining the subthalamic-nucleus (STN) in Parkinson's disease (PD). Positive therapeutic response devoid of poor side effects to STN-DBS for PD depends to a high degree on lead position in the STN. The sensorimotor area of the STN (which is a preferred-location), lies dorsolaterally, in a part discernible by discrete beta (β) oscillations (frequency-band 13Hz–30Hz) in the Parkinsonian state. We present an objective real-time method (whose throughput is very maximal) to precisely differentiate sub territories of the STN in stereotactic-functional-neurosurgery, based on MERs and statistical signal/image processing probabilistic hidden Markov models (HMMs). In this study. Fifty two MER trajectories were employed, attained 21 PD patients who underwent bilateral STN-DBS functional-neuro-surgery for electrode-implantation. The offline Mat-Lab utility tools, such as, root mean square (RMS) and fast Fourier transform (FFT) discrete Fourier transform (DFT) hamming window based power spectral density (PSD) of the MER signal recordings were utilized to train and test the Markov-model in discovering the dorsolateral oscillatory area (DLOA) and non-oscillatory ripples (non-harmonics) sub-territories within the subthalamic-nuclei. The model discriminations were compared to the decisions of a skilled-end-user. The HM-model identified STN-entry, ventral boundary of DLOA, and STN-exit with an error -0.09 ± 0.35 , -0.27 ± 0.58 , and -0.20 ± 0.33 mm (mean \pm SD), and with finding reliability with less than 1mm error of 94.95%, 85.94%, and 91.21%. The model was thriving despite a very uncouth grouping method and was brawny of hefty to parameter-variation. Hence, by using Markov(HM) model in concurrence with RMS and PSD measures of intra-operative MER-signal can give enhanced classiness/or elegance of STN entry and exit in disparity with earlier methods, and introduces a new (intra-operative-STN) finding of a DLOA ventral-limit. We hypothesized the MER trajectory by means of Markov-hidden-model.

Key Words: Beta Oscillatory Activity(BOA), Deep brain stimulation(DBS), Dorsolateral Oscillatory Area(DLOA) Fast Fourier Transform (FFT), Hidden Markov Model (HMM), Microelectrode Recording (MER), Parkinson's Disease (PD), Power Spectral Density (PSD), Subthalamic-Nuclei (STN), Tremor Frequency Oscillations (TFOs)

1. INTRODUCTION

One of the of the most commonest neurodegenerative disorders that elders' experience, Parkinson's disease (PD) is a critical diagnosis affecting approximately 2 of every 1,000 older adults [1], which is characterized by the hall mark cardinal motor symptoms, namely, tremor, Bradykinesia, rigidity and postural instability. Although there is currently no cure and current PD management help alleviate only the features or symptoms rather than the disease's progression, fresh hope lies in new research focused on neuro-protection. PD, the causes of which are unknown, is a chronic, progressive brain disorder that belongs to a larger class of disorders called movement disorders. The search for optimal cure is on for the past 2 centuries since the time it was first described by James Parkinson [2]. In PD, one particular population of brain cells—those that produce a chemical messenger called dopamine—become impaired and are lost over time. "The loss of these brain cells causes' basal-ganglia (BG, an important organ or part of brain) circuits in the brain to function exceptional, and those exceptional circuits result in human movement and motor control problems [1].

The STN-DBS for advanced idiopathic Parkinson's disease (PD) has proven to be harmless, effective for motor symptoms, valuable, and the therapeutic efficacy is the primary goal of DBS [3]-[5]. During surgery for implanting DBS electrode in STN, microelectrode recording (MER) is often utilized to physiologically pinpoint the STN [6]-[8], predictive role in terms of the response to STN-DBS, to identify the MER signal characteristic discharge patterns (signatures) of STN that correlate with improved motor symptoms of PD as well as movement-related activity (MRA). To implant the macroelectrode successfully within the optimal position (probably the sensorimotor part of the STN) [9], accurate demarcation of the PD patient's (subject's) STN (based on the MERs) is required. This includes derivation of the entry and exit points of the STN across the MER trajectory, as well as localization of the sensorimotor area within the STN.

It has been well established that the STN can be divided into three (sensorimotor, limbic, and cognitive/associative) functional territories, each broadly involved in its respective basal ganglia-thalamo-cortical loop [10]-[15]. The sensorimotor area of the STN is primarily positioned dorsolaterally [16]-[19], the same lay that

seems to provide optimal therapeutic benefit to subjects undergoing STN DBS [20]-[23]. Furthermore, it has been shown that local field potential (LFP) [24]-[26] and single unit [27] (when averaged across subjects) beta-oscillatory-activity (BOA) is generated largely within the dorsolateral portion of the STN. It would therefore seem that there is correspondence between the dorsolateral oscillatory area (DLOA) and the sensorimotor area of the STN, and that beta-oscillatory activity could possibly predict the most effective contact for STN DBS [28], [29]. The extent of this overlap (DLOA, sensorimotor STN area, and optimal DBS location), however, still requires further investigation. The approach of this paper is a reliable, real-time objective method that can be applied to a single STN MER diffusion. Such a method could assist the neurosurgeon for implanting electrode in the optimal location or simply be used to estimate the transitions of a MER trajectory. Automatic methods have been described to identify the entry and exit points of the STN [30]-[33]. We present a real-time objective method (whose throughput is very maximal) to set the limits of the outer boundaries of the STN as well as an intra-operative-STN (DLOA-ventral) boundary during surgery based on the root mean square (RMS) and fast Fourier transform (FFT) based power spectral density (PSD) of the MERs, using Markov hidden model which are originally designed by [34], [47], [48].

1. Baterials and methods

1.1 Targeting STN with Magnetic Resonance Imaging

The target nucleus for the DBS surgery is STN. The problem with targeting subthalamic nucleus is that it is an almond shaped small biconvex lens structure and not clearly identified on the diagnostic MR imaging scanner due to lack of contrast between the STN and the surrounding structures [35], [36]. The STN can be visualized on the MRI but other methods such as Lozano's technique where a position 3 mm lateral to the superolateral border of the red nucleus is targeted have been studied and found to be effective areas for stimulation [37]. As the MRI techniques are not absolutely perfect, use of electrophysiological techniques such as microelectrode recording from the subthalamic nucleus as well as intra-operative stimulation have helped in clearly distinguishing the STN. Microelectrode recording can identify subthalamic neurons by their characteristic bursting pattern and their signals clearly identify the subthalamic-nucleus from the surrounding structures. On table stimulation is studied to ensure that the three is optimal benefit with the least side effects and this is the final test to ensure the correct targeting of the STN.

1.2 Microrecordings

The recordings from 21 PD subjects (i.e., patients) undergoing bilateral STN DBS electrode implantation were analyzed. All subjects met the conditions accepted

selection criteria for implantation and signed informed consent for surgery with MER signal recording. Ethical clearance was approved by NIMS Hospital (AP State University Act 1989). All the subjects were anesthetized locally and awake during-surgery throughout the surgery. Data were obtained off dopaminergic medications and during periods of rest. For both the right and left hemispheres, a single trajectory using one or two channel electrodes (separated by 2 mm anteroposteriorly in the parasagittal plane) was made starting at 10 mm above the computed target. The electrodes were advanced in small discrete steps, toward the estimated center of the lateral STN. Step size was tamed by the neurologist in order to attain optimal unit signal acquisition and detection of upper and lower borders of the STN. Typically, shorter steps (100 μ m) were used when the electrode was advanced closer to the presumed location of the STN. Following a 2-second (2mV calibration) signal stabilization period after electrode movement cessation, multi-unit traces were acquired for the duration of 5 seconds. Each dataset consists of MER signals acquired—recorded from all depths of five-probes.

1.3 Signal Recording

Signal processing and signal analysis methods were performed using the Mat-Lab technical computing. The MER signals were filtered with band-pass filters and adaptively band-stop filtered to reject 50 Hz noise occurring from mains line frequency. The adaptive filter applied here employed the power ratio of the stop-band and of reference sidebands to adjust attenuation of the stop-band to avoid over or under filtering.

1.3.1 Signal characteristics of STN and SN

According to neurologists, the signal characteristics of the target nuclei STN are [46]:

- A increase in the background noise
- An increased density high rate neuronal discharge
- An irregular high rate neuronal activity (bursting activity)

Because of the high neuron discharge rate occurring in STN region, the amplitude of background-signal increases significantly. As the electrode entered SN area, the high firing rates are observed as well. However, the characteristics of firing pattern are no more irregular bursting but periodic firing.

2.3.2 Root Mean Square

In computational simulation mathematical bio-statistical signal processing and its applications, the root mean square (RMS) is defined as the square root of the mean square which is the arithmetic mean of the squares of a set of numbers [3]. It is also referred to as the quadratic-mean and is a particular case of the generalized mean with $e=2$

exponential. It can also be referred to for a continuously varying function in terms of an integral of the squares of the instantaneous values during a cycle. The entry and exit from the subthalamic-nuclei are marked primarily by a vivid increase and decrease in normalized RMS (i.e., nRMS), correspondingly [31], [34], [34]. In addition, PSD can be used as a marker for the dorsolateral oscillatory area of the subthalamic-nucleus based on the increased BOA. The normalized root-mean-square and spectrum (the power spectral density) of an example trajectory, as a function of estimated distance to target (EDT), are depicted in Figure 1.

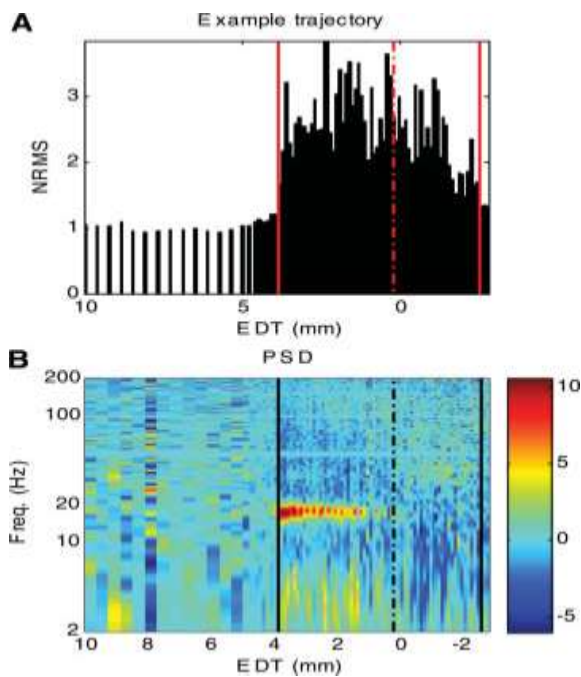


Figure 1 A. The nRMS of an example trajectory (Case/Subject S17, right-side hemisphere STN) as a function of estimated distance to target (EDT). (B) The PSD of the same trajectory. The PSD color-scale represents $10 \times \log_{10}$ (PSD power/average PSD power) per EDT. The red (A) and black (B) solid vertical lines indicate STN entry and exit; the dot-dash lines indicate the ventral boundary of the dorsolateral oscillatory area (DLOA).

1.4 Computation of PSD

The power spectral density (PSD) is used to compute nonparametric PSD estimates equivalent to the periodogram using fast Fourier transform (FFT). The FFT is an algorithm to compute the discrete Fourier transform (DFT) with less number of additions and multiplications [49]. The examples show how to properly scale the output (o/p) of FFT for even length inputs (i/p, i.e., data points), for normalized frequency (in hertz or cycles/second), and for one and two sided PSD estimates. While plotting the PSD, 50 Hz (Indian English channel) interference from mains lines power supply (ripples or artifacts) and their harmonics were replaced by the mean PSD, and the PSD

was smoothed in the frequency direction using a narrow Hamming window (standard deviation $\sigma = 0.33$ Hz). The PSD spectrum was computed with 1 s sliding window, 0.5 seconds overlap and 4096 data—points. Resting PSD was normalized across all contact pairs of a given electrode at each frequency. The normalized power of contact pair C_i on the frequency f_i was computed using the following equation

$$P_{\text{Normalize}}(C_i, f_j) = \frac{P(C_i, f_j)}{\frac{1}{3} \sum_{i=1}^3 P(C_i, f_j)}$$

2.5 Hidden markov Models

Hidden Markov models [46], [47], [48] are used to estimate the position of the electrode at each depth across the trajectory based on the nRMS and PSD of the microelectrode-recordings. In this, four discrete states are defined: Prior to the subthalamic-nuclei, in the dorsolateral oscillatory area (DLOA) of the STN, in the non-oscillatory STN, and finally out of the STN. A typical trajectory state chain or sequence would go through all four states consecutively. However, not all trajectories had oscillatory recordings (ORs) in the presumed dorsolateral area of the STN; hence, a trajectory could skip state 2. In addition, it was possible for a trajectory to end in state 3 (a MER trajectory that was terminated before exiting the STN). In the advancement of a sequence, it was possible to remain in the same state, however not likely to go backwards (for instance, from a state within the STN to prior to the STN state). Trajectories that did not pass through the STN were not included in this study because they are a trivial case for which the RMS remains at the electrical baseline level through the trajectory and there are no transitions. An HMM state sequence uniquely defined three possible state transitions:

1. In – STN entry (noted by transition from state 1 to state 2 or state 3).
2. Dorsolateral oscillatory area (DLOA) ventral – the ventral boundary of DLOA
3. Out – STN exit (noted by transition from state 3 to state 4)

The design of possible Markov states and their corresponding transitions is depicted in Figure 2.

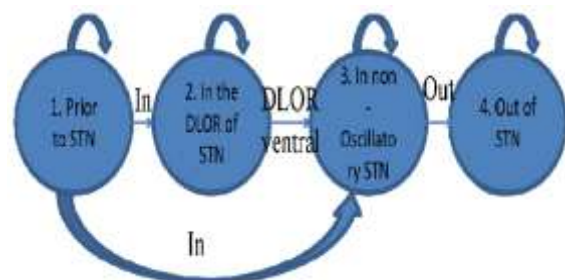


Figure 2. Four possible hidden Markov model States and transitions. The arrows-indicates the 3 possible states and transitions.

2.6 Data Observations and Grouping

Parzen [45] derived very good estimator. The best estimator is “consistent” and “unbiased”.

Consistency: An estimator is said to be unbiased if its expected value is identical with the population parameter being estimated. As the sample size increases gets closer to $\hat{\theta}$ gets closer to θ

$$\lim_{n \rightarrow \infty} p(|\hat{\theta} - \theta| > \epsilon) = 0 \text{ is “consistent”}.$$

$$E[\hat{\theta}] = \theta \text{ is “unbiased”}.$$

Sampling distribution of $\hat{\theta}$ should have a small standard error is “precise”. These are the three probabilistic models that are employed in order get the estimation. The following paradigm gives the bias versus precision:

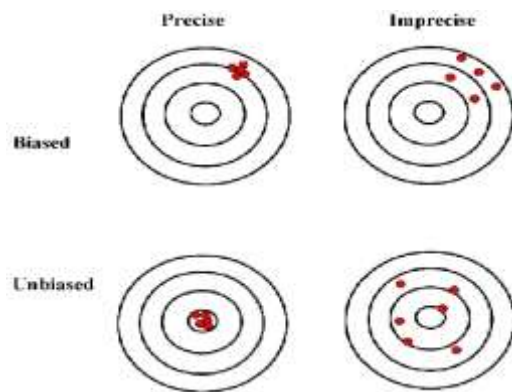


Figure 3 Bias versus precision

Unbiasedness: If an estimator, say θ , approaches the parameter θ closer and closer as the sample size ‘n’ increases, θ is said to be a consistent estimator of θ . To best estimate the Markov hidden-state, the following observations were used in this study.

1. The normalized root mean square (nRMS)
2. The mean beta (13Hz–30 Hz) PSD
3. The maximum beta PSD

Since the data set was limited (52 trajectories), it was necessary to have a relatively small HMM emission matrix (the matrix depicting the probability of each observation per HMM state) else it would not be adequately sampled during the learning stage. This requirement limited the resolution with which the three different observation quantities could be quantized since the number of possible combinations defines the order of the matrix. A custom method uncouth (yet logical, as will be explained below) quantization was adopted, whereby the observations were grouped into six clusters as follows:

All observations with nRMS < 1.25 (threshold 1), i.e. below a 25% increase from the nRMS electrical baseline (which is equal to 1 due to the normalization) were grouped together (*Low-nRMS* group). The mean deviation from threshold 1 (i.e. nRMS - 1.25) of the remaining observations was computed. Threshold 2 was defined by threshold 1 and 25% of the computed mean deviation. Observations with nRMS between threshold 1 and threshold 2 were grouped together (*Intermediate-nRMS* group), while observations with nRMS > threshold 2 were further divided according to their (maximum and mean) BOA (above or below the median), resulting in a further four (*high-nRMS*) groups.

The reasoning behind the cluster-analysis can be explained as follows: In conglomerating the nRMS, using an absolute threshold (1) was appropriate since the RMS was normalized. Albeit, there exists inter-patient-variability (IPV) of nRMS within the STN; therefore in addition to each particular trajectory. The nRMS > threshold 2, the observations were further grouped based on the PSD since the DLOA ventral transition (based on PSD), takes place at high values of nRMS, i.e., within the STN. It was noted that some subjects had narrow band of BOA (e.g., Figure 1B), where as others had a wider band (for instance, Figure 4A). We presumed that maximum and mean beta PSD would better capture narrow and wide band beta oscillations, correspondingly. Both mean and maximum (BOA) were used for PSD grouping. Tremor frequency oscillations (TFOs) seemed to be episodic [27] and sporadic. They were not always present and when present they did not define a continuous area as the beta oscillations did (Figure 4A). We therefore we did not incorporate into the HMM.

2.7 Estimating Hidden Markov Models

For each trajectory, the “known” state transitions were defined (corresponding to the three possible HMM state transitions—mentioned earlier in section The Hidden Markov model). In (*STN-entry*) and Out (*STN-exit*) transitions were based on intra-operative neuronal analysis by the neurophysiologist as well as the nRMS plots and the DLOA-ventral transition was distinguished by visual inspection of the PSD, noting a sudden diminish in BOA. The known state transitions are depicted in the NRMS plots by red-lines and in the PSD plots by black lines (Figures. 1 and 4). These transitions from one state to other states defined a known state cycle for estimating and testing the HMM.

The maximum likelihood estimate of the HMM transition and emission probability matrices were estimated based on the known state sequences. Since the training data were fully labeled (there were known state sequences for the whole data-set), there was no need for the expectation-maximization (EM) algorithm or iterative procedures in the manner of heuristics trial and error-

based (which would require initial guessing of the probability matrix values), and the matrices values could be directly estimated.

2.8 Testing Hidden Markov Models

After the HMM was estimated using the known state sequences of all trajectories excluding one (N 2 1 5 55), we then tested on the excluded trajectory (with no assumption of its sequence) by evaluating the deduced HMM state transitions to the trajectory's known state transitions. The deduced HMM state sequence was computed as the most probable sequence beginning with the HMM in state 1 before the first observation (using [34]). This process was repeated N (52) times, individually testing each trajectory. The mean and SD of the error in estimating each of 3 transitions were computed.

2.9 Hardware

The following hardware is employed in this study. Medtronic 5 channel MER machine, DBS system battery (Medtronic) with input impedance <250 Ωs. Extracellular single/multi-unit MER was performed with microelectrode 291 with 10µm width (Medtronic); impedance 1.1±0.4 MΩ, and a 16-bit analogue to digital converter (A/DC).

2.10 Software

The following software is used in this study. The data analysis was carried out on custom-built software developed by us, Mat-Lab Version 9.2 using with Markov models utility tool-box.

We analyzed fifty two trajectories. In our analysis, individual trajectories established the existence of a distinct DLOA boundary but not gradient (Figures 1B and 4A). Some trajectories had a short DLOA where as others had a longer DLOA and when puddled the varied trajectories standard to a gradient of BOA. Hence, it is suggested that each trajectory has a divergent boundary that can be visually discerned and automatically detected by an HMM. In nutshell, there is a divergent dorsolateral oscillatory range.

For each of the 52 trajectories, the HMM was estimated individually based on the other 51 trajectories. The HMM cycle state of the trajectory being tested was then deduced using [34], based on the trajectory's grouped *nRMS* and *PSD* sequence. Figure 4 shows a typical trajectory's *PSD* (Figure 5A) and *nRMS* (Figure 5B) as well as the mean and maximum BOA used for grouping (Figure 5C). Figure 3D presents the tags resulting from grouping (blue-line) together with the HMM deduced state sequence (green-line). The deduced state transitions are noted by the steps in the state sequence (e.g. a step from state 1 to state 2 signify the transition is in, etc.). In this example, the HMM transition inference concurs with the known in

transitions and out transitions (solid red-lines), but slightly precedes the known DLOA-ventral transition (dot-dash red-line). For each transition (In, out, and DLOA-ventral) the state transition error was defined (the validity) as follows:

$$Error = S - \hat{S}$$

Where, S is the known state transition (which is observed) defined by the neurologist and \hat{S} is the Markov's deduced state-transition (Figure 4, red-lines and steps in the green-line, correspondingly) in EDT. Hits and rejections or correct rejections (R, or CRs) were the number of properly identified and suitably annulled transitions correspondingly. Hits did not take into account detection accuracy, it was simply used to count the number of deduced HMM transitions where there was also a known transition. However, all hits, were within 2mm, and 88% of hits were within 0.5mm of the known transitions (Figure 5).

Missing rates were the number of transitions that the HMM did not detect and False Alarms (FAs) were the number of HMM transition detections when by specialist decision there was no transition. A histogram of the spatial errors in deducing the location of the state transitions can be seen (Figure 4) and an outline of the results (including Hits, CRs, FAs, and Misses) can be seen (Table 2). Detection reliability (Table 2) was computed by the sum of correct detections (Hits 1 CRs) divided by the total number of trajectories. In transition error described here (mean ±SD: -0.09 ±0.35mm was better than that found by the Bayesian method [27]-[29] both in mean and SD (Bayesian method, error 5 0.18 6 0.84 mm). The Out transition error (mean 6 SD: 20.20 6 0.33 mm) also demonstrated better mean and standard deviation (Bayesian method, error 5 0.50 6 0.59 mm). The DLOA ventral transition detection is novel and therefore doesn't have a reference for comparison, but showed similar results to the in and out detections (mean 6 SD: 20.27 6 0.58 mm). HMM algorithm Steve J Young [48] had to deal with a heterogeneous variation of trajectories. While achieving good results despite this challenge (Table 2 and Figure 5), it failed on event. Nonetheless, the HMM proved to be a robust. This was tested both by varying the detection thresholds (up ↑ and down ↓) and also by removing the stability analysis. Minimal or no-effect of these variations was seen on detection accuracy and reliability, demonstrating robustness of the model.

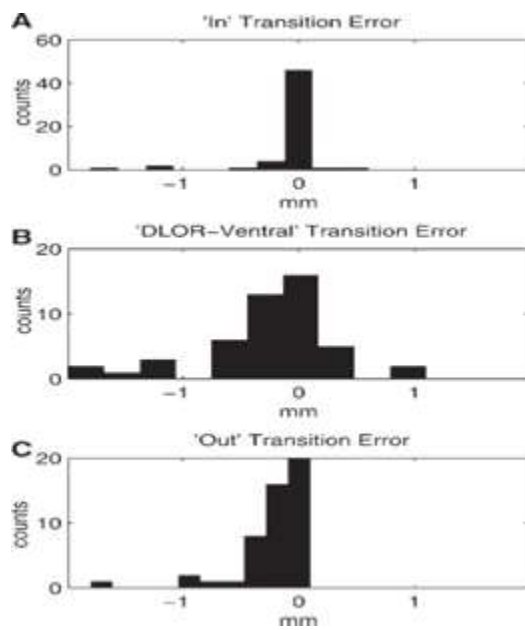


Figure 5. The HMM transition error histograms for A, in (B). DLOA-ventral, and in (C) Out state transitions.

Figure 5 and outline of the results (including Hits, R or CRs, FAs, and Misses. See Table 2). Detection reliability was computed by the sum of correct detections (Hits 1 CRs) divided by the total number of trajectories (Table 2). See Table 2 for the computation of detection reliability (limiting hits to those with error < 1mm).

3. CONCLUSIONS

positive effects of lead-position with microelectrode signal recording of bilateral STN DBS on motoric symptoms and quality of life have been demonstrated in 21 subjects with advanced idiopathic Parkinson's disease cases, albeit adverse effects of non-motoric features like cognitive impairment, cognitive dementia, axial symptoms like slurred speech, hallucinations, cognitive deterioration or psychiatric complications have also been reported. Since the STN has separate sensorimotor, limbic, and cognitive/associative subterritories, it would seem probable that accurate implantation of the DBS electrode within the sensorimotor area is essential for attaining therapeutic motor benefit while avoiding limbic or cognitive side effects. Hence, differentiation of the outer boundaries of the STN is inadequate, and separation of the subterritories of the STN is required. With this model it likely to probable for delineation of subterritories within the subthalamic-nuclei.

In this study, a simple and hierarchical but elegant (and uncouth) clustering technique offered excellent state hypothesis of the MER trajectory by means of Markov model. Enhanced accuracy than the Bayesian method for discovering STN entry/exit was attained, with the addition of an intra-STN DLOA-ventral transition detection. The HMM state space representation models can be used off-

line to automatically detect the trajectory state transitions (one state to other state), or semi or quasi-online at the end of a trajectory during STN DBS to aid delicacy discrimination of the sensorimotor STN for implantation of electrode. The limit of DLOA-ventral transition can assist the neurosurgeon in deciding which MER channel or pathway to implant, when multiple and parallel electrodes are used for 5 channel Medtronic parallel MER machine, and in implanting the macroelectrode at the optimal depth. Positive therapeutic benefit to STN-DBS has been associated with proximity of the active electrode contacts to the dorsolateral border of the STN [20], [21], [23]. It has been proposed that this may be due to activation of adjacent structures such as the zona incerta and/or fields of Forel. It is likely suggested that the benefits of STN dorsolateral border implantation of electrode may also be due to avoidance of volume conduction to ventral areas, which have been connected with neuro-electro-psychological side-effects [42], [43]. If this is the case then electrode distance from the DLOA-ventral border may be of primary importance in attaining optimal sensorimotor benefit without cognitive or limbic side-effects. Our results show that higher resolution, computed across enormous data set, in concurrence with a more complex Markov models utilizing spike phase—shape and discharge pattern probably may even give improved results which can be done in future and microrecording can discover STN by their characteristic bursting signal pattern (or signatures) and their signals clearly identify the nucleus from the surrounding structures. The only lacuna with the process of MER signal assessment is it may increase the subjects' (the PD patients) yoke (if awakened). A discussion on latest in PD is explained elaboratively and extensively in Appendix.

APPENDIX

Discussion on neuroprotection - latest in science - analysis of Parkinson's disease

Neuroscientists particularly those who are conducting research for a new discovery [1], [3]-[44] have found that, in many of the cases, the presence of PD appears to be erratic or chaotic—haphazard, even-though some risk factors have been identified, with the greatest being age, followed by genetics and environment. "While genetic risk factors are being defined, the genetics of Parkinson's disease are not yet fully coherent or lucid. However most scientists do think it is a convolution of genetics and environment, where as some researchers think that the combination of genetics and environment may speed up a normal aging trajectory truly. There are some people who say that if everyone lived to be 110 years, we would all have Parkinson's disease or Alzheimer's—that this is an aging brain and that somehow the trajectory has sped up [1]. Scientific—neuroresearchers are not quite sure about that and say that 'it is not rationale'. We do know that there is damage at some point or lack of function of these

dopamine cells at some point in life, but we are not sure where it is or for how long it goes on since as it is scientifically not proved. The early signs of the disease means through prediction – prognostic diagnosis may help us understand the progress of the disease because it is more than just these cells in the brain; it influences other cells as well that we are learning more and more regularly. More men than women are afflicted with PD, and “other risk factors seem to be people who live in developed countries or in a rural environment, and the rural environment has been linked to possible exposure to pesticides [44]. The average age of PD onset is about 60, and the risk increases with age. Why is that the case? This is an area of research emphasis, as scientists are not certain [44]. “One theory suggests that the disease process begins long before symptoms become evident and that a younger, more plastic brain is able to recompense and function relatively normally for some amount of time. Our human brain is, one of the world’s biggest mysteries yet to be wholly tacit, an incredibly complex organ and can possibly deal with some small blips in the system; however, the aging process may lessen the ability to balance, larger numbers of dopamine neurons are lost, and classic disease symptoms emerge.”

A 1. Symptoms and prognostic diagnosis

Movement problems are a classic sign of PD and be able to differ amongst individuals in prevalence and severity. Each person may have one or more of these features (i.e., motoric--

Symptoms), some slightly worse than others. The PD motoric symptoms are: tremor, stiffness (e.g., elders’ limbs or bodies become more rigid), Bradykinesia (e.g., elders start to move very slowly), and postural instability (e.g., impaired balance). Initial symptoms of PD can be so sly that subjects frequently simply mistake them for facets of normal aging. Initially, symptoms might be really trivial [43]. Someone might notice that their handwriting gets smaller, that their hand starts to shake (and also cramps in case of other movement disorders like Writer’s cramp), that they may have more difficulty standing up, or that they are a little unsteady or slow (postural instability). Now, most of those things are something we might think would happen as we get older, but what starts to happen is they become gradually worse, and they start to affect daily activities—things like talking speaking, moving walking, eating, or reading a newspaper or when hand reaching for a cup of coffee. At that point, that is when people usually visit the doctor. There are also common symptoms that often precede the motor signs of PD, including insomnia (difficulty in sleeping); changes in sense of aroma—smell; fatigue; restless legs; and constipation.

There is quite a bit of research right now going on into what these early signs might mean and if that could help predict an improved diagnosis and treatment of the

disorder [1], [44]. A PD diagnosis is usually guided by presenting symptoms as there is no blood or other test to identify the disease. Although one might think a brain scan such as an MRI may be successful in detecting concerned organs or elements or components (STN neurons in SN) in PD patients, in a scan like magnetic resonance imaging, which shows structural changes in the brain, they appear normal in Parkinson’s disease because these cells that die off are a very tiny population, yet they have a huge impact on the PD subject’s movement [3], [44]. Diagnosis can also be complicated by the fact that other disorders can have similar symptoms to those exhibited with PD. After older adults are put on PD treatments for their symptoms, a more definitive judgment can be made. “Parkinson’s disease may be difficult to diagnose initially, albeit the classic PD symptoms and response to medications are supportive factors [1].

A 2. Management – Then and Now

The balance of management for PD is individualized because older adults can have varying degrees of symptoms, and no two subjects react in exactly the same way [44]. The gold standard for treating PD, which has been used for many years as its primary treatment, is Levodopa (the metabolic precursor of dopamine). A type of dopamine-replacement therapy, “It’s a compound that is naturally found in plants and animals, and it’s a precursor to dopamine,” noting that it is typically given with another compound called carbidopa to ensure its ability to cross the blood-brain barrier and get into the brain. When it gets into the brain, the brain cells convert L-dopa into dopamine, which reduces the tremor symptom and some of the motoric symptoms and allows the subjects to lead relatively normal lives and that L-dopa (a precursor to metabolic dopamine) does not facilitate with balance and other non-motoric symptoms (such as cognitive dementia, cognitive impairment, speech, hallucinations, and axial symptoms). Albeit, that L-dopa can create its own problems. One thing that happens with L-dopa is that, as subjects are on it for a longer duration of time, they start to have side effects called dyskinesias, which are abrupt involuntary movements noting that they can influence older adults’ quality of life. Imagine you are having a really hard time walking and this drug makes it better, but suddenly you get these very strange movements. One of the challenges facing therapeutic development for PD is discovering the means to restore and improve motor function and decrease involuntary movements while maintaining quality of life for the individual and providing as full a range of motion as possible.

According to [1], there are different categories of dopamine-replacement drugs that, by targeting different parts of the dopamine metabolic pathway as L-dopa does, increase the production of dopamine [3]-[44]. Compounds such as Azilect, a monoamino oxidase B inhibitor, can block the degradation of dopamine, and still others

enhance the activity of dopamine at its receptor (the dopamine signal). These drugs all fundamentally improve dopamine signaling in the brain to aid the dented circuits.

Another category of drugs is used to balance other brain chemicals that are also affected after the dopamine cells die, and there is also a other class of drugs that will have an effect on the non-motoric symptoms subjects with PD may experience, such as anxiety, depression, and orthostatic hypotension, etc.

For subjects whose symptoms are minimally improved by medication, deep brain stimulation has been implemented and has become a successful treatment for some PD patients because it may reduce the need for medication and improve dyskinesias. Evidence suggests that deep brain stimulation significantly improves movement and quality of life in PD subjects. Consultation with a physician is necessary to determine whether this surgical procedure is the best course of action for an individual PD patient.

A 3. Expectations in neuroprotection

Even though several managements and medications are being utilized for older adults with PD, all the contemporary medications work on managing symptoms, but none of these medications stop the disease's progression. New research into neuro-protection is trying to change that. Neuroprotection is where research is headed right now because L-dopa, as far as we know, does not stop the progression of the disease. None of the drugs that are available impede the progression. Hence, there is maximum endeavor in this area right now in both basic research and clinical trials. Neuroprotection has researchers looking down new avenues for a cure, such as dietary supplements and drugs that have been used in the treatment of other movement disorders. For instance, several ongoing clinical trials are examining the effects of creatine, which is commonly used to build muscle, and coenzyme Q10, which works through cellular structures called mitochondria, the power plants of cells, to clear any harmful substances that are produced if the mitochondria are not working to capacity. For example, if a power plant were releasing hazardous chemicals into the atmosphere, coenzyme Q10 would serve as a filter to prevent this from happening and keep the environments clear, allowing those around to breathe and inhale and exhale better.

Both of these compounds are neuroprotective in animal models and have been well tolerated in humans, so, there is significant focus on using dietary and nutritional supplements and drug-medicines that have been utilized for other disorders that in animal models have an effect, for stopping the progression of PD. Isradipine as an example of compound researchers are currently studying. Isradipine makes old dopamine cells young again by changing the pattern of communication of these cells with brain circuits. [1] Conducting clinical research to

determine whether isradipine and similar compounds will improve the function of dopamine cells and provide a new therapy for PD." Other clinical trials are now examining urate's effect on PD. "A large study has shown that high levels of urate may actually be protective in Parkinson's disease." There are many studies ongoing in this area right now, both at basic research and clinical trial levels [1], [43], [44]. A cure for PD can be expected any day now, no one knows how close—or far away—that cure may be. However, there is a great deal of high-quality directed, focused research that is currently being funded by the National Institutes of Health, National Institute of Mental Health (NIMH) and nonprofit foundations, such as the Michael J. Fox Foundation, Parkinson's Disease Foundation, National Parkinson Foundation, Lasker Foundation, Pratiksha Trust/ Infosys (India), Edmond J. Safra Fellowship in Movement Disorders, to bring that date closer for all those who suffer from the disease. Scientists have made rapid progress in defining potential causes of PD [1]. Currently, significant efforts in basic and clinical research are directed toward development of disease prediction and improved treatments, including the identification of neuroprotective strategies able to slow disease progression. As scientists continue to find out more about the function of genes, risk factors, and brain circuits involved in PD, they work steadily toward a cure.

A 4. Hypothesis

Evidently neuroprotection is the new cutting-edge in movement disorders research and therapeutic—treatment. The long-term clinical studies have so far botched to establish that high-frequency stimulation has been able to slow down the progression of the disease [44]. So-called 'earlystim' clinical protocols have only proven that it was safe to stimulate STN much earlier than it was so far accepted. At the experimental level, Benabid [44] has published that in MPTP-treated monkeys, high-frequency stimulation of the STN could protect neurons in the substantia-nigra (SN). To test this hypothesis in humans, one would need to perform STN stimulation at the very beginning of the disease, which is not easily ethically sustainable given the surgical possibility, even if low, in subjects who are still minimally impaired by the disease [44].

ACKNOWLEDGMENT

The authors wish to thank the Dept of Science & Technology (DST) for the Cognitive Science Research Initiative CSRI Project Grant [# SR/CSRI/201/2016] funded by the DST, Ministry of Science & Technology (MST), Govt of India (GoI), New Delhi.

REFERENCES

1. Peter J, Neurodegeneration and neuroprotection in Parkinson's disease, Academic press, Edi.3, London, 2018
2. Parkinson J, An Essay on Shaking Palsy, Sherwood, Neely and Jones: London, 1817.
3. Limousin P, Pollak P, Benazzouz A, et al. Bilateral subthalamic nucleus stimulation for severe Parkinson's disease. *Mov Disord* Vol. 10, Pp: 672-674, 1995.
4. Krack P, Batir A, Van Blercom N, et al. Five-year follow-up of bilateral stimulation of the subthalamic nucleus in advanced Parkinson's disease. *N Engl J Med*, Vol. 349, Pp: 1925-1934, 2003.
5. Machado A, Rezai AR, Kopell BH, Gross RE, Sharan AD, Bena-bid AL. Deep brain stimulation for Parkinson's disease: surgical technique and perioperative management. *Mov Disord*, Vol. 21, Pp: S247-S258, 2006.
6. Sterio D, Zonenshayn M, Mogilner AY, et al. Neurophysiological refinement of subthalamic nucleus targeting. *Neurosurgery*, Vol. 50, pp: 58-67, 2002.
7. Israel Z, Burchiel K. Microelectrode recording in movement disorder surgery. Stuttgart: Thieme; 2004.
8. Gross RE, et.al, Electrophysiological mapping for the implantation of deep brain stimulators for Parkinson's disease and tremor. *Mov Disord*, Vol. 21, Pp: S259-S283, 2006.
9. Starr PA. Placement of deep brain stimulators into the subthalamic nucleus or Globus pallidus internus: technical approach. *Stereotact Funct Neurosurg*, Vol. 79, Pp: 118-145, 2002.
10. Alexander GE, Crutcher MD, DeLong MR. Basal ganglia-thalamo-cortical circuits: parallel substrates for motor, oculomotor, "pre-frontal" and "limbic" functions. *Prog Brain Res*, Vol. 85, Pp: 119-146, 1990.
11. Parent A, Hazrati LN. Functional anatomy of the basal ganglia. II. The place of subthalamic nucleus and external pallidum in basal ganglia circuitry. *Brain Res Brain Res Rev*, Vol. No. 20, Pp: 128-154, 1995.
12. Shink E, Bevan MD, Bolam JP, Smith Y. The subthalamic nucleus and the external pallidum: two tightly interconnected structures that control the output of the basal ganglia in the monkey. *Neuroscience*, Vol. No. 73, pp: 335-357.
13. Joel D, Weiner I. The connections of the primate subthalamic nucleus: indirect pathways and the open-interconnected scheme of basal ganglia-thalamocortical circuitry. *Brain Res Brain Res Rev*, Vol. 23, Pp: 62-78, 1997.
14. Hamani C, Saint-Cyr JA, Fraser J, Kaplitt M, Lozano AM. The subthalamic nucleus in the context of movement disorders. *Brain*, Vol. 127, Pp: 4-20, 2004.
15. Baup N, Grabli D, Karachi C, et al. High-frequency stimulation of the anterior subthalamic nucleus reduces stereotyped behaviors in primates. *J Neurosci*, Vol. 28, Pp: 8785-8788, 2008.
16. Monakow KH, Akert K, Kunzle H. Projections of the precentral motor cortex and other cortical areas of the frontal lobe to the subthalamic nucleus in the monkey. *Exp Brain Res*, Vol. 33, Pp: 395-403, 1988.
17. Nambu A, Takada M, Inase M, Tokuno H. Dual somatotopical representations in the primate subthalamic nucleus: evidence for ordered but reversed body-map transformations from the primary motor cortex and the supplementary motor area. *J Neurosci*, Vol. 16, Pp: 2671-2683, 1996.
18. Rodriguez-Oroz MC, Rodriguez M, Guridi J, et al. The subthalamic nucleus in Parkinson's disease: somatotopic organization and physiological characteristics. *Brain*, Vol. 124, Pp: 1777-1790, 2001.
19. Romanelli P, Esposito V, Schaal DW, Heit G. Somatotopy in the basal ganglia: experimental and clinical evidence for segregated sensorimotor channels. *Brain Res Brain Res Rev*, Vol. 48, Pp: 112-128, 2005.
20. Herzog J, Fietzek U, Hamel W, et al. Most effective stimulation site in subthalamic deep brain stimulation for Parkinson's disease. *Mov Disord*, Vol. 19, Pp: 1050-1054, 2014.
21. Godinho F, Thobois S, Magnin M, et al. Subthalamic nucleus stimulation in Parkinson's disease: anatomical and electrophysiological localization of active contacts. *J Neurol*, Vol. 253, pp: 1347-1355, 2006.
22. Coenen V, et.al, What is dorso-lateral in the subthalamic Nucleus (STN)?—a topographic and anatomical consideration on the ambiguous description of today's primary target for DBS surgery. *Acta Neurochir*, Vol. 150, Pp: 1163-1165, 2008.
23. Moks CB, Butson CR, Walter BL, Vitek JL, McIntyre CC. Deep brain stimulation activation volumes and their association with neurophysiological mapping and therapeutic outcomes. *J Neurol Neurosurg Psychiatry*, Vol. 80, Pp: 659-666, 2009.
24. Kuhn AA, Trottenberg T, Kivi A, Kupsch A, Schneider GH, Brown P. The relationship between local field

- potential and neuronal discharge in the subthalamic nucleus of subjects with Parkinson's disease. *Exp Neurol*, No. 194, Pp: 212–220, 2005.
25. Weinberger M, Mahant N, Hutchison WD, et al. Beta oscillatory activity in the subthalamic nucleus and its relation to dopaminergic response in Parkinson's disease. *J Neurophysiol*, No. 96: Pp: 3248–3256, 2006.
26. Trottenberg T, et.al, Frequency-dependent distribution of local field potential activity within the subthalamic nucleus in Parkinson's disease. *Exp Neurol*, No. 205, Pp: 287–291, 2007.
27. Moran A, Bergman H, Israel Z, Bar-Gad I. Subthalamic nucleus functional organization revealed by Parkinsonian neuronal oscillations and synchrony. *Brain*, No. 131, Pp: 3395–3409, 2008.
28. Marsden JF, et.al. Subthalamic nucleus, sensorimotor cortex and muscle interrelationship in Parkinson's disease. *Brain*, No. 124, Pp: 378–388, 2011.
29. Chen CC, Pogosyan A, Zrinzo LU, et al. Intra-operative recordings of local field potentials can help localize the subthalamic nucleus in Parkinson's disease surgery. *Exp Neurol*, No. 198, 214–221, 2006.
30. Falkenberg JH, McNames J, Favre J, Burchiel KJ. Automatic analysis and visualization of microelectrode recording trajectories to the subthalamic nucleus: preliminary results. *Stereotact Funct Neurosurg*, No. 84, Pp: 35–44, 2006.
31. Moran A, et.al, Real-time refinement of subthalamic nucleus targeting using Bayesian decision-making on the root mean square measure. *Mov Disord*, No. 21, Pp: 1425–1431, 2006.
32. Novak P, et.al, Detection of the subthalamic nucleus in microelectrographic recordings in Parkinson disease using the high-frequency (>500 Hz) neuronal background: technical note. *J Neurosurg*, No. 106, Pp: 175–179, 2007.
33. Rabiner LR. A tutorial on hidden markov models and selected applications in speech recognition. *Proc IEEE*, No.77, Pp: 257–286, 1999.
34. Zaidel A, et.al, Prior pallidotomy reduces and modifies neuronal activity in the subthalamic nucleus of Parkinson's disease subjects. *Eur J Neurosci*, Vol. 27, Pp: 483–491, 2008.
35. Ashkan K, et.al, Variability of the subthalamic nucleus: the case for direct MRI guided targeting. *Br J Neurosurg*. Vol. 21(2), Pp: 197–200, April 2007.
36. Patel NK, et.al, Comparison of atlas- and magnetic-resonance-imaging-based stereotactic targeting of the subthalamic nucleus in the surgical treatment of Parkinson's disease. *Stereotact Funct Neurosurg*. Vol. 86 (3), Pp: 153–61, 2008.
37. Andrade-Souza, et.al, Comparison of three methods of targeting the subthalamic nucleus for chronic stimulation in Parkinson's disease. *Neurosurgery*. No.62, Suppl 2 :875–83, Feb 2008
38. Danish SF, et.al, Determination of subthalamic nucleus location by quantitative analysis of despiked background neural activity from microelectrode recordings obtained during deep brain stimulation surgery. *J Clin. Neurophysiol.* No.25, Pp:98–103, 2008
39. Deuschl G, et.al, A randomized trial of deep-brain stimulation for Parkinson's disease. *N Engl J Med* Vol. 355, Pp: 896–908, 2006.
40. Saint-Cyr et.al. Neuropsychological consequences of chronic bilateral stimulation of the subthalamic nucleus in Parkinson's disease. *Brain*. No. 123, Pp: 2091–2108, 2000.
41. Voon V, Kubu C, Krack P, Houeto JL, Troster AI. Deep brain stimulation: neuropsychological and neuropsychiatric issues. *Mov Disord* Vol. 21, Pp: S305–S327, 2006.
42. Bejjani BP, Damier P, Arnulf I, et al. Transient acute depression induced by high-frequency deep-brain stimulation. *N Engl J Med* Vol. 340, Pp: 1476–1480, 1999.
43. Herzog J, Reiff J, et al. Manic episode with psychotic symptoms induced by subthalamic nucleus stimulation in a subject with Parkinson's disease. *Mov Disord* Vol. 18, Pp: 1382–1384, 2003
44. Alim L. Benabid, *Nature Medicine*, Vol. 20, No. 10, Pp: xviii–xx, Oct 2014.
45. James B, Remi B, Algorithms for Hyper-Parameter Optimization, <https://papers.nips.cc/paper/4443-algorithms-for-hyper-parameter-optimization.pdf>
46. S Wong, et.al, Functional localization of visualization of the subthalamic nucleus from microelectrode recordings acquired during DBS surgery with unsupervised machine learning, *Journal of Neural Engineering*, 2009.
47. M. Gales and S. Young, *The Application of Hidden Markov Models in Speech Recognition*, *Foundations and Trends in Signal Processing*, Vol. 1, No. 3, Pp: 195–304, 2007, c2008, DOI: 10.1561/20000000004

48. Steve J Young, Philip C. Woodland, State clustering in hidden Markov model-based continuous speech recognition, *Journal of Computer speech and language*, Cambridge university, 1994, DOI: 10.1006/csla.1994.1019.
49. Cooley, Tukey, An algorithm for machine calculation of complex Fourier series. *Math. Comput.* Vol.19, Pp: 297–301, 1965.

BIOGRAPHIES



Venkateshwarla **Rama Raju** received the B.Sc.(Hon`s), post B.Tech (Hon`s), M.Tech, and PhD all in India. He also pursued an Advanced MS Degree through research in Cognitive Science (AI/Medical-Neuroscience, Neural computing Neural systems, Natural Language and Speech Processing, Speech Technology & Auditory - Processing) at ILASH-Research Centre, Computer Science Dept, University of Sheffield (England,1994-95), M.Phil/D.Sc. Degree in Biomedical-Signal-processing from the Bioengineering-Transducers-Signal-Processing(BTSP) Research Group of University of Leicester (UoL) Dept of Engg (England,1995-97), worked as Scientist/Engineer at Planning Commission (New Delhi) through Indian Engineering Services (IES), Research Fellow at UoS and UoL. Presently, he is a full Professor at CMRCET Hyderabad involved in developing and applying new estimation, systems and control-tools in order to: build computational simulation and statistical models of electrical-activity in neural-circuits affected by Parkinson`s disease, understand electrophysiological-dynamics of neural-circuits in health/disease-states during DBS treatment, design more effective, adaptive, and safer DBS-strategies for neurological-neurodegenerative-disorders.



Anuradha Boya received her B.Tech (CSE) from Sri Krishnadevaraya University affiliated and M.Tech (CSE) from JNTUA affiliated. Presently she is working as an Associate Professor in the Dept of CSE, CMRCET, Hyderabad. In parallel, she is also pursuing a PhD in CSE from BENNETT University, Greater Noida Uttar Pradesh. She published 5 articles in International Journals till now in particular IEEE Intelligent systems, etc.